UCRL 3106

UNIVERSITY OF CALIFORNIA

Radiation Laboratory

TWO-WEEK LOAN COPY

This is a Library Circulating Copy which may be borrowed for two weeks. For a personal retention copy, call Tech. Info. Division, Ext. 5545

BERKELEY, CALIFORNIA

DISCLAIMER

This document was prepared as an account of work sponsored by the United States Government. While this document is believed to contain correct information, neither the United States Government nor any agency thereof, nor the Regents of the University of California, nor any of their employees, makes any warranty, express or implied, or assumes any legal responsibility for the accuracy, completeness, or usefulness of any information, apparatus, product, or process disclosed, or represents that its use would not infringe privately owned rights. Reference herein to any specific commercial product, process, or service by its trade name, trademark, manufacturer, or otherwise, does not necessarily constitute or imply its endorsement, recommendation, or favoring by the United States Government or any agency thereof, or the Regents of the University of California. The views and opinions of authors expressed herein do not necessarily state or reflect those of the United States Government or any agency thereof or the Regents of the University of California.

UCRL-3106

UNIVERSITY OF CALIFORNIA

Radiation Laboratory
Berkeley, California

Contract No. W-7405-eng-48

PROTON-INDUCED FISSION CROSS SECTIONS FOR U^{238}, U^{235}, Th^{232}, Bi^{209}, and Au^{197} at 100 to 340 Mev

Herbert M. Steiner and John A. Jungerman

August 24, 1955

Printed for the U. S. Atomic Energy Commission

PROTON-INDUCED FISSION CROSS SECTIONS FOR U^{238}, U^{235}, Th^{232}, Bi^{209}, and Au^{197} at 100 to 340 Mev

Herbert M. Steiner

Department of Physics, Radiation Laboratory,
University of California, Berkeley, California

and

John A. Jungerman

Department of Physics,
University of California, Davis, California

August 24, 1955

ABSTRACT

We have measured the total fission cross sections of U^{238}, U^{235}, Th^{232}, Bi^{209}, and Au^{197} for high-energy protons. A cancellation-type ionization chamber was used to detect the fission fragments. The observed fission cross sections are compared to the total inelastic cross sections in order to obtain the relative fission probability as a function of proton energy.

PROTON-INDUCED FISSION CROSS SECTIONS FOR U^{238}, U^{235}, Th^{232}, Bi^{209}, and Au^{197} at 100 to 340 Mev.

Herbert M. Steiner

Department of Physics, Radiation Laboratory,
University of California, Berkeley, California

and

John A. Jungerman

Department of Physics
University of California, Davis, California

August 24, 1955

I. INTRODUCTION

In recent years several experiments have been carried out in the general field of high-energy proton-induced fission in heavy elements.[1,2,3,4] Most of these experiments were designed primarily to measure the mass yield distribution of fission products as a function of the energy of the bombarding particles. In some cases the yields were integrated to give total fission cross sections; however, these were usually subject to rather large errors because of uncertainty in absolute counting of beta activities and also in beam monitor calibration. The experiment described here was designed to measure the total fission cross sections of U^{238}, U^{235}, Th^{232}, Bi^{209}, and Au^{197}, using a cancellation-type fission chamber to detect the ionization produced by the fission fragments. It was considered of interest to compare these fission cross sections with the total inelastic proton cross sections for the above elements in order to determine how the fission probability changed as a function of the energy of the incident protons.

The source of protons used in this experiment was the 184-inch synchrocyclotron at the University of California Radiation Laboratory. The cross sections were measured in the energy region from 100 to 340 Mev.

II. APPARATUS

A. Fission Detector

A cancellation-type ionization chamber of 2π geometry filled with 1 atmosphere of hydrogen gas was used to detect the fission fragments. This type of fission chamber was first used by Baldwin and Klaiber,[5] and was independently suggested by Clyde Wiegand and used by John Jungerman[1] for charged-particle fission studies. As shown in Fig. 1, it consisted of three electrodes, A, B, and C, arranged so as to form two adjacent parallel-plate ionization chambers of approximately equal capacitance. The spacing between the electrodes was 4.5 centimeters, and under usual operating conditions plate A was operated at zero potential, plate B at about +1500 volts, and plate C at about +3300 volts. Electrode B, which served as the high-voltage electrode of chamber B-C, was coupled by means of a 100 μμf capacitor to the grid of the first tube of a preamplifier. When equal amounts of ionization were produced simultaneously in both regions A-B and B-C, the net signal on electrode B could be made less than one percent of the ionization pulse from one region alone. A beam of charged particles passing through the fission chamber produced almost equal amounts of ionization in both these regions if care was taken to make the electrodes as thin as possible. The high-voltage electrodes were therefore made out of 140 $\mu g/cm^2$ of aluminum foil. The degree of cancellation could be adjusted by varying the high voltage on electrode C. This affected the saturation in the region B-C, so that under optimum conditions almost complete cancellation of the pulses caused by the beam ionization could be obtained. (See Figs. 2 and 3.) Upon achievement of the best possible cancellation, a sample of fissionable material was placed in the beam at electrode A. The ionization produced by a fission fragment did not cancel for two reasons: (a) the range of a fission fragment in hydrogen is about 7 to 9 cm,[6] so that most of the fragments spent all of their range in the region A-B; (b) a fission fragment ionizes most heavily at the beginning of its path, so that even if the fragment were to get into the cancellation region B-C, it would already have lost most of its energy in the region A-B. The beam usually entered the chamber in the direction C-B-A, so that most of the reaction products made by the beam in the 0.001-inch aluminum sample backing were knocked out of the sensitive part of the ionization chamber. Approximately four times as many background pulses

were observed when the orientation of the chamber was reversed. A periodic check was made of the cancellation and background by inserting a blank piece of 0.001-inch aluminum foil in place of the fissionable sample. The number of background beam pulses remained quite constant for a given beam intensity at a given energy, and thus could be subtracted with good reliability. The number of such background pulses was less than 1 percent of the number of fission pulses for U^{238}, U^{235}, and Th^{232}, less than 10 percent of the number of bismuth fission pulses, and less than 25 percent of the number of fission pulses from gold for all proton energies.

The signal from the preamplifier was fed into a linear pulse amplifier that had a clipping time of 5 microseconds. From there it was distributed into six scalers whose voltage discriminators were set at 5, 7.5, 10, 12.5, 15, and 20 volts respectively under usual operating conditions. In this way a counting-rate-versus-bias curve was obtained at each point. (See Fig. 4.) The true counting rate was obtained by extrapolating this curve to zero bias.

The pulses recorded as fission pulses in this experiment were observed to have the same form and magnitude as slow-neutron-induced fission pulses. Such pulses were observed with the above-described chamber when a Po-Be source encased in paraffin was placed adjacent to the fission chamber with the U^{235} sample in place.

B. Samples

The samples were prepared by either painting or evaporating the fissionable materials onto pieces of 0.001-inch aluminum foil. The areas of all samples were about 2 by 2 inches. The painting technique is described elsewhere.[7,8,9] The thickness of each sample was determined by both alpha counting and weighing whenever possible, and by weighing only for bismuth and gold. To check for uniformity in alpha-active samples all but a 0.75-cm^2 area of each sample was masked, and the exposed part of the sample was then alpha counted. The emission of alpha particles was measured with an ionization chamber from about six regions on the surface of each sample. The alpha activity in all cases was found to be uniform to within ± 3 percent. For U^{238} both painted and evaporated samples were prepared and used. No difference was observed between the cross sections for the painted and evaporated samples. Also, for uranium, a quantitative chemical analysis of two samples was made which showed agreement, within the

experimental error of 3 percent, with the thicknesses as determined by alpha counting. All the targets used ranged in thickness from 0.6 to 1.1 mg/cm^2. In order to correct for sample thickness effects, thinner samples of U^{238}, Th, Bi, and Au were also prepared. These samples ranged from 0.1 to 0.4 mg/cm^2 in thickness. Cross sections were measured by using these thin samples at a proton energy of 336 Mev. These results were compared with the cross sections as measured with the thicker samples. In this way sample-thickness correction factors were determined for the thicker samples. It was assumed that these sample-thickness corrections were independent of the energy of the proton beam. The sample-thickness correction factors used in these experiments ranged between 8 and 14 percent.

C. Beam Monitor

The beam was monitored by a parallel-plate ionization chamber filled with one atmosphere of argon. This method of monitoring the beam is described in detail by Chamberlain, Segrè, and Wiegand.[10] The accuracy of the beam calibration using the above method is estimated to be ± 3 percent.

III. EXPERIMENTAL METHOD

A. Arrangement

The general experimental arrangement is shown in Fig. 5. The high-energy protons were magnetically deflected out of their circular orbits in the 184-inch synchrocyclotron, and passed through a premagnet collimator, a steering magnet, and a collimator 1-inch in diameter by 48 inches long into the experimental area (cave). The full-energy proton beam was essentially monoenergetic, with a probable energy spread about the mean of less than 1 percent. To reduce the energy of the beam, internal absorbers were placed on a movable probe that could be positioned so that all the beam from the magnetic channel had to pass through these absorbers. Beryllium was used as the absorbing material in order that the multiple Coulomb scattering effects could be kept small, thus keeping the beam intensity as high as possible. The current to the focusing magnet was then adjusted so as to guide the reduced-energy particles down the 48-inch collimator. The steering magnet also acted as a momentum selector, and thus reduced the energy spread introduced by range straggling in the absorbers. Upon entering the cave the beam first passed through the monitoring ionization chamber (No. 1) and then through the

fission chamber. The beam next passed through a variable copper absorber and finally through a second ionization chamber (No. 2). From the ratio of the charge collected in ion chamber No. 2 to the charge collected in ion chamber No. 1, with various amounts of copper absorber in between the chambers, a Bragg curve was obtained, and hence the energy of the beam could be determined.

B. Procedure

1. Alignment

The alignment of the fission chamber was checked with photographic film. These pictures were taken every time the current in the steering magnet was changed.

2. Variation of High Voltage on Electrodes B and C

Under usual operating conditions the high voltage on electrode B was +1500 volts. If this voltage was changed to 1000 volts (with a simultaneous reduction of the voltage on electrode C, so that cancellation was maintained), the slope of the integral bias curve would increase; however, the extrapolated end point at zero bias would remain the same within statistics. Conversely, when the voltage on B was increased to +2000 volts, the slope of the bias curve decreased but the end point was still unchanged. (See Fig. 4.) Unfortunately, when the voltage on electrode C was set at values above 4000 volts, occasional spark breakdowns occurred which registered as fission pulses. We therefore decided to operate electrodes B and C at +1500 and +3300 volts respectively.

3. Pile-up of Fission Pulses

The 184-inch synchrocyclotron has a repetition rate of 60 pulses per second, and each pulse of the scattered beam has a duration of 20 microseconds. These 20-microsecond pulses have a radiofrequency fine structure; however, this fine structure is of no importance to us, since the resolving time of the electronic equipment used in conjunction with the fission chamber was 5 microseconds. In order to keep the loss of fission events due to pile-up of fission pulses to less than 1 percent, we chose the beam intensity so as to give less than 300 fission counts per minute. This number was determined by making a curve of the counting rate per microcoulomb of charge collected on the beam-monitoring ionization chamber, versus the reciprocal of the beam intensity. Such a curve is shown in Fig. 6. No change was observed in either the total number of observed fission pulses or the shape of the integral

bias curves when the clipping time of our amplifier was changed from 5 microseconds to 1 microsecond.

4. Gating of Scalers

In order to minimize the effects of pulses due to electrical disturbances in the cyclotron building, an electronic gate was employed that allowed the scalers to count only while the beam was on. This was helpful because occasionally electrical transients would cause spurious pulses to be detected during the 5-microsecond resolving time of our electronics when the gate was not used. In order to insure that no fission counts were being lost because of the gating procedure, the gating circuit could be switched so as to allow the scalers to count only during the time that the beam was not on. No counts above background were ever observed.

5. Geometry of the Fission Chamber

The geometry of the fission chamber was tested by placing an alpha standard in place of one of the fissionable samples on the ladder-shaped frame in the chamber. The diameter of the alpha standard was about 1.25 inches, which was approximately equal to the beam size at the targets when the chamber was used at the cyclotron. Upon comparison of the counting rate of the alpha standard as measured in the fission chamber with the counting rate as measured in an ionization chamber whose geometry was strictly that of flat parallel plates, it was found that 1.5 ± 0.5 percent fewer counts were observed in the fission chamber. This is presumably because the ladder-shaped frame would position the sample approximately 1/32 inch behind electrode A. Hence, the effective solid angle was slightly less than 2 π steradians.

6. Neutrons

The neutron contamination of the beam was checked by placing sufficient copper absorber to completely stop the proton beam immediately in front of the fission chamber. This check probably overestimated the neutron contamination, because of the additional neutrons produced by the protons in the copper absorber. In any case the fissioning effect of these neutrons was less than 1 percent of the proton-induced fission rate for all samples except U^{235}. For U^{235} this effect was approximately 2 percent.

7. Momentum Transfer to Struck Nucleus

The usual orientation of the fission chamber was chosen in such a way that the fission fragments were observed in the backward hemisphere with

respect to the beam direction. Since a fission fragment is a rather slowly moving object (e.g., an 80-Mev fission fragment of A = 100 has $\beta = 0.04$, where β is the velocity of the fragment divided by the velocity of light), a small amount of momentum transferred to the target nucleus appreciably distorts the angular distribution of the fission fragments in the laboratory system. For example, if a 340-Mev proton were to transfer all of its momentum to a target nucleus of U^{238}, then the target nucleus, which is the center-of-mass frame for the fission fragments, would have $\beta = 0.0039$. If we assume (a) that the fission fragments are emitted isotropically in their center-of-mass system, and (b) that we have a thin sample, then the motion of the fissioning nucleus would cause about 10 percent fewer fragments to enter the sensitive region of the ionization chamber than when the fission occurs with the nucleus at rest. In other words the center-of-mass motion causes the effective solid angle available to the detected fission fragments to be reduced by 10 percent, when the beam passes through the chamber in the direction C-B-A. On the other hand, if the orientation of the chamber is ABC with respect to the beam direction, 10% more fragments enter the sensitive region of the ionization chamber. However, no increase in the counting rate is observed, since only one pulse will be detected, whether it is caused by only one fragment or by both fragments emitted simultaneously.

If (a) we have a sample of finite thickness in which a fraction η of the fragments is self-absorbed when the fission occurs with the nucleus at rest, and if (b) there is a fractional change ξ in the effective solid angle due to the center-of-mass motion then if the beam direction is CBA the fraction of the fissions observed in our chamber is $1-\eta-\xi$. On the other hand, if the beam direction is ABC, this fraction is approximately $1 - \eta + \xi - \frac{\xi^2}{4\eta}$ for $0 < \xi < 2\eta$, and 1 for $\xi > 2\eta$. In this experiment we had $\xi < 2\eta$ in all cases. Hence, by taking the ratio of the fissions observed when the chamber is oriented in the direction CBA to the fissions observed when the chamber is oriented in the direction ABC, we can determine ξ; i.e.,

$$\frac{CBA}{ABC} = 1 - 2\xi + \frac{\xi^2}{4\eta} .$$

It was noted that at $E_p = 336$ Mev approximately 7 ± 3 percent fewer fissions were observed in the backward hemisphere (with respect to the beam) than in the forward direction. This corresponds to $\xi = 0.037 \pm .011$. Since

$$\xi = \frac{\beta \text{ (target nucleus)}}{\beta \text{ (fission fragment)}} ,$$

β (target nucleus) $\cong 0.037 \times 0.04 = 0.0015$, which implies that on the average approximately one-third of the proton's initial momentum is transferred to the uranium nucleus. At a proton energy of 192 Mev, $\xi = 0.020 \pm .012$, which again corresponds to a momentum transfer of approximately one-third of the proton's initial momentum.

Besides the difference in the number of fission events observed when the orientation of the chamber was changed by 180°, we also found that the slope of the integral bias curves was steeper when the fissions were observed in the backward direction with respect to the beam than in the forward direction. An effect of this kind is again consistent with the interpretation that an appreciable amount of momentum is transferred to the fissioning nucleus.

IV. RESULTS

The fission cross sections of U^{238}, U^{235}, Th^{232}, Bi^{209}, and Au^{197} as a function of proton energy are presented in Figs. 7 through 11. Only standard deviations due to counting statistics are indicated on the graphs. In addition to the statistical errors the following systematic errors may be ascribed to the experiment: (a) determination of sample thickness, ± 3 percent; (b) uniformity of sample thickness over the area of the sample, ± 3 percent; (c) self-absorption of fission fragments in the sample material, ± 5 percent; (d) extrapolation to zero bias, ± 5 percent; (e) momentum transfer to the target nucleus, ± 1.5 percent; (f) determination of beam energy, ± 1 percent; (g) calibration of beam monitor, ± 3 percent; (h) geometry of the chamber, ± 0.5 percent. When these errors are compounded, a total systematic error of 9 percent may be ascribed to the experiment. The accuracy of the absolute cross sections may be obtained by combining the above systematic errors with the errors due to counting statistics shown in Figs. 7 through 11.

V. DISCUSSION

Upon comparing the fission cross sections to the total inelastic cross sections as measured by attenuation experiments,[11] we find that for U^{238} and U^{235} fission is the most probable inelastic process at all energies investigated. A graph of the ratio of the fission cross section to the total inelastic cross section as a function of proton energy is shown in Figs. 12 and 13. For uranium bombarded by 340-Mev protons the difference between the total inelastic cross section of about 1.75×10^{-24} cm^2 and the fission cross section of 1.35×10^{-24} cm^2 is approximately 0.4×10^{-24} cm^2. This value is not in disagreement with a chemical determination of the spallation cross section of U^{238} bombarded with 340-Mev protons.[12]

The results of this experiment are significantly higher than those obtained by one of us (J. A. J.) in an earlier experiment.[1] The reason for this discrepancy is not entirely clear. However, we believe that the results given here are correct and the old ones in error; a possible reason for assuming the earlier work to be in error is that it was done with an electrically deflected proton beam which had pulses of about 0.1 microsecond duration. This small-duty-cycle beam created a much larger amount of ionization in the fission chamber during the resolving time of the fission detector than in the newer experiment. These large bursts of ionization may have caused the ion chamber used in the previous experiment to operate unreliably.

The present cross section for U^{238} at 147 Mev is about 12 percent below that obtained by Harding.[2] Chemical investigations of the fission yields of U^{238} when bombarded by 340-Mev protons have been carried out by Folger, et al.[3] Upon integrating these yields they find a fission cross section of 2.0×10^{-24} cm^2, which is somewhat higher than the result reported here.

The bismuth fission cross section at 340 Mev as measured in this experiment is in fair agreement with the value of $0.239 \pm .03 \times 10^{-24}$ cm^2 obtained by Biller[4] by integration of the fission yields.

The following conclusions may be drawn from this experiment:

(a) The high-energy fission cross sections of uranium seem to be independent of whether U^{235} or U^{238} is used.

(b) The relative fission probabilities as well as the fission cross sections seem to decrease strongly with decreasing atomic number.

(c) The fission cross sections of uranium and thorium seem to be fairly constant as a function of proton energy in the energy region of 100 to 340 Mev.

(d) On the average approximately one-third of the proton's initial momentum is transferred to the fissioning nucleus at proton energies of 190 and 340 Mev.

VI. ACKNOWLEDGMENTS

We wish to thank Professor Emilio Segrè for suggesting this experiment, and for his continuous interest during the course of the experiment. Thanks are also due to Professor Owen Chamberlain and Dr. Clyde Wiegand for their helpful suggestions and for interesting discussions. The samples were prepared and analyzed with the cooperation and help of Daniel J. O'Connell, Larry Williams, and Richard Sinnott. The help of Donald Keller, John Baldwin, David Fischer, and James Simmons during the runs is also greatly appreciated. Finally, the entire cyclotron crew under the direction of Mr. James Vale is to be thanked for their smooth operation of the cyclotron.

This work was performed under the auspices of the U. S. Atomic Energy Commission.

References

1. J. Jungerman, Phys. Rev. 79, 632 (1950).
2. G. N. Harding, AERE/NR-1438.
3. R. L. Folger, P. C. Stevenson, G. T. Seaborg, Phys. Rev. 98, 107 (1955).
4. W. F. Biller, "The Characteristics of Bismuth Fission Induced by 340-Mev Protons" (Thesis), University of California Radiation Laboratory Report No. UCRL-2067, Jan. 1953.
5. G. G. Baldwin and G. S. Klaiber, Phys. Rev. 71, 3 (1947).
6. N. O. Lassen, Phys. Rev. 75, 1762 (1949).
7. T. Jorgensen, MDDC-467 (1946).
8. W. C. Bright, MDDC-91 (1946).
9. B. B. Rossi and H. H. Staub, "Ionization Chambers and Counters", McGraw-Hill, N.Y., (1949) pg. 210.
10. O. Chamberlain, E. Segrè, C. Wiegand, Phys. Rev. 83, 923-932 (1951).
11. G. P. Millburn, W. Birnbaum, W. E. Crandall, and L. Schecter, Phys. Rev. 95, 1268-1278 (1954).
12. M. Lindner, private communication.

Figure Captions

Fig. 1. Schematic drawing of the cancellation-type ionization chamber used to detect the fission fragments.

Fig. 2. Photograph showing typical pulses observed in an oscilloscope during various stages of cancellation of the pulses due to beam ionization. The cancellation of the beam pulses was adjusted by varying the voltage on electrode C with respect to electrodes A and B.

(a) A = 0 volts, B = 1500 volts, C = 1750 volts; beam pulse largely uncancelled

(b) A = 0 volts, B = 1500 volts, C = 3000 volts; beam pulse almost cancelled

(c) A = 0 volts, B = 1500 volts, C = 3290 volts; minimum beam signal

(d) A = 0 volts, B = 1500 volts, C = 4500 volts; beam pulse reappears with opposite sign.

A fission pulse on same scale would be approximately 2 cm high on the oscilloscope (full scale ~4 cm).

Fig. 3. Voltage on electrode B (collector) versus voltage on electrode C (cancellation) in order to achieve the best possible cancellation of pulses caused by beam ionization in the fission chamber.

Fig. 4. Integral bias curves for various voltages on the collector electrode (electrode B). Electrode C was always adjusted to give the best possible cancellation of beam pulses. (See Fig. 3).

Fig. 5. Schematic diagram of the experimental arrangement at the cyclotron. (The representation of the experimental equipment in the cave is not to scale.)

Fig. 6. Counting rate plotted against the reciprocal of the beam intensity. The ordinate shows the number of counts observed while the beam monitor collected 1 microcoulomb of charge. The abscissa shows the time necessary to charge the beam monitor to 1 microcoulomb.

Fig. 7. Fission cross section of U^{238} as a function of proton energy. The errors indicated on the points are standard deviations due to counting statistics only.

Fig. 8. Fission cross section of U^{235} as a function of proton energy. The errors indicated on the points are standard deviations due to counting statistics only.

Fig. 9. Fission cross section of Th^{232} as a function of proton energy. The errors indicated on the points are standard deviations due to counting statistics only.

Fig. 10. Fission cross section of Bi^{209} as a function of proton energy. The errors indicated on the points are standard deviations due to counting statistics only.

Fig. 11. Fission cross section of Au^{197} as a function of proton energy. The errors indicated on the points are standard deviations due to counting statistics only.

Fig. 12. Ratio of the fission cross sections σ_f of U^{238}, U^{235}, and Th^{232} to the total inelastic cross section of natural uranium σ_i. The total inelastic cross sections were obtained from the data of Millburn et al.[11] The shaded regions indicate the limits of error.

Fig. 13. Ratio of the fission cross sections σ_f of Bi^{209} and Au^{197} to the total inelastic cross section of lead, σ_i. The total inelastic cross sections were obtained from the data of Millburn et al.[11] The shaded regions indicate the limits of error.

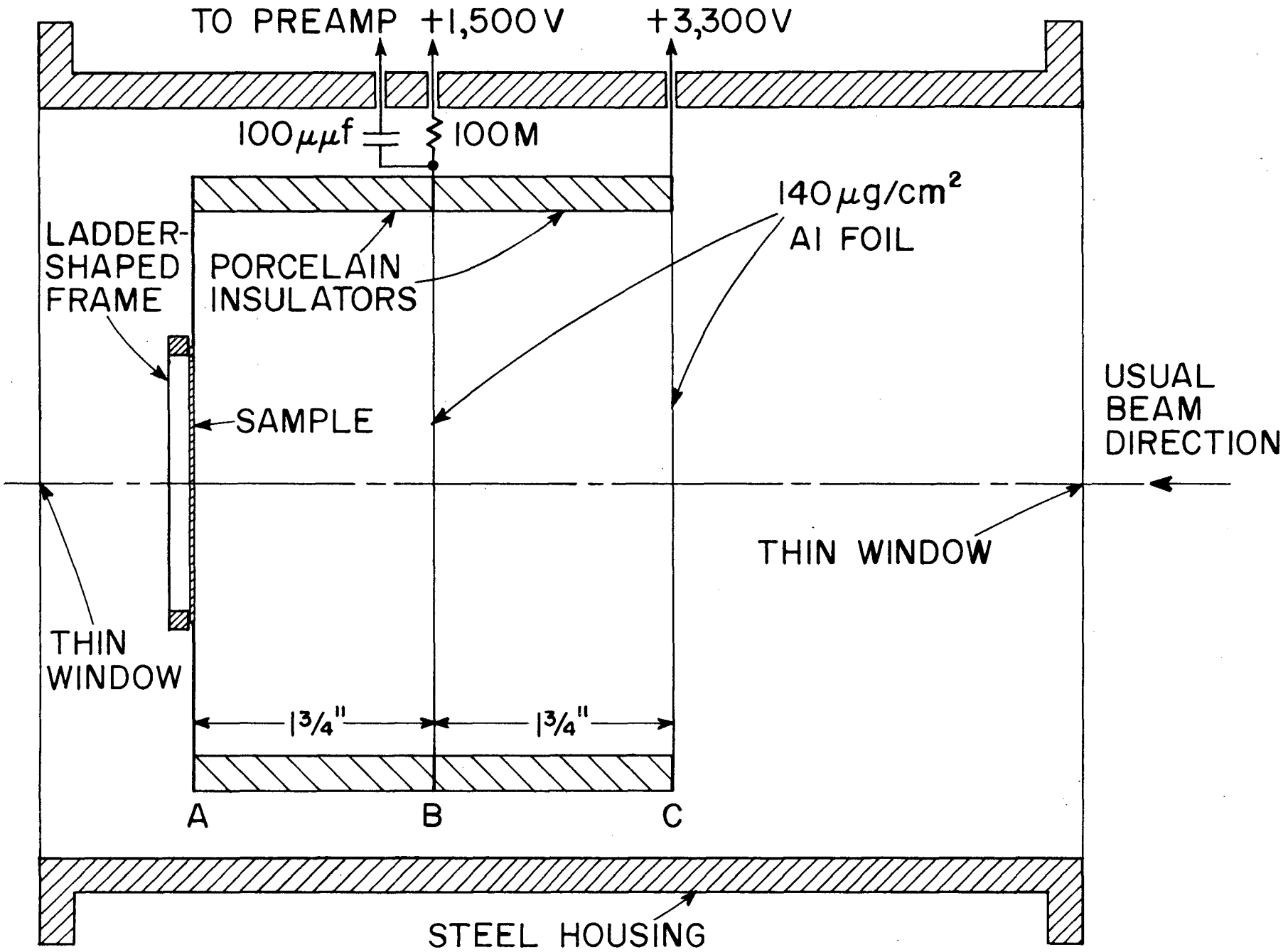
TO PREAMP
+1,500V
+3,300V
100μμf
100M
140μg/cm²
Al FOIL
LADDER-SHAPED FRAME
PORCELAIN INSULATORS
SAMPLE
USUAL BEAM DIRECTION
THIN WINDOW
THIN WINDOW
1 3/4"
1 3/4"
A
B
C
STEEL HOUSING

Fig. 1.

23945-1

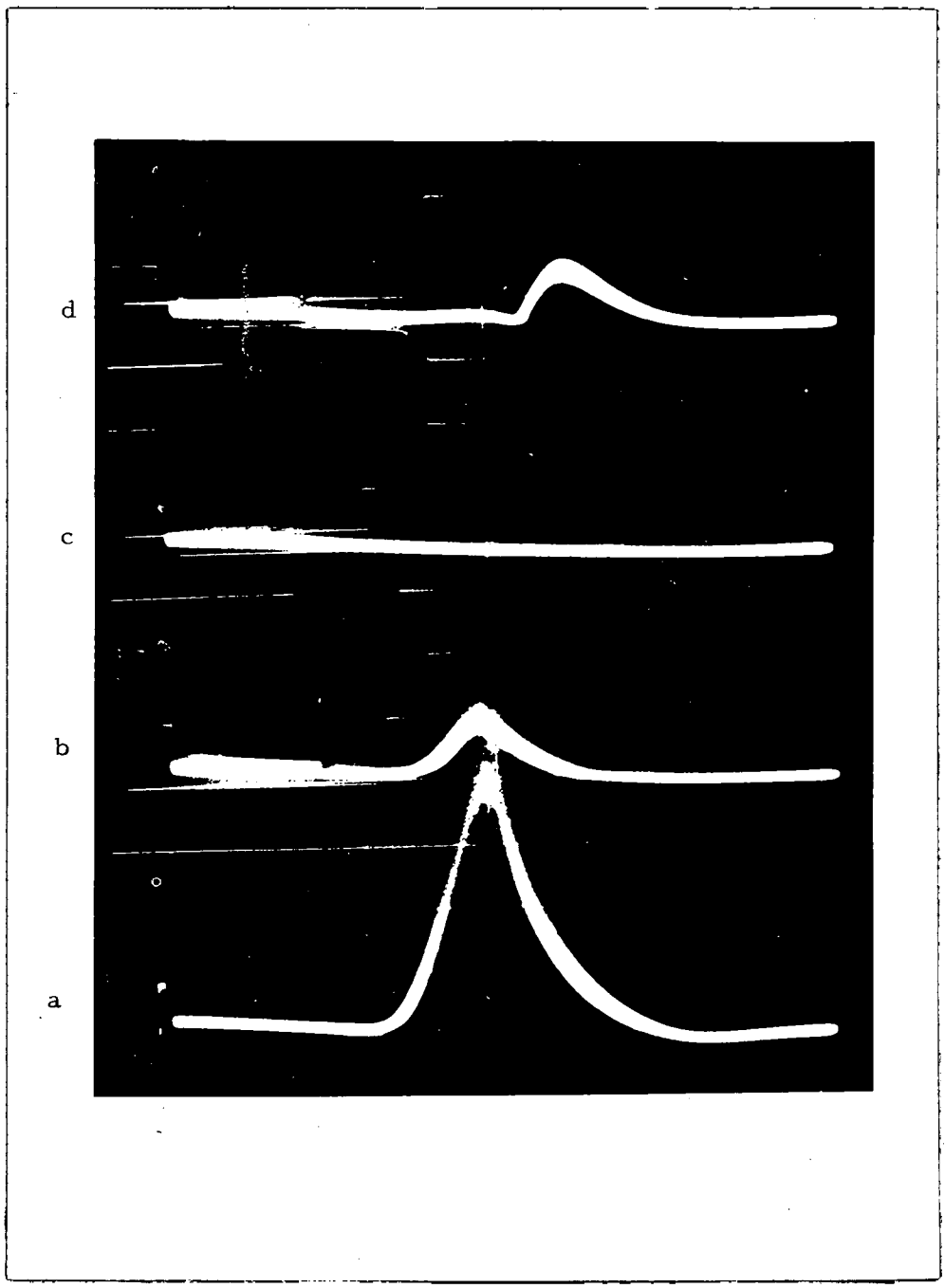

Fig. 2

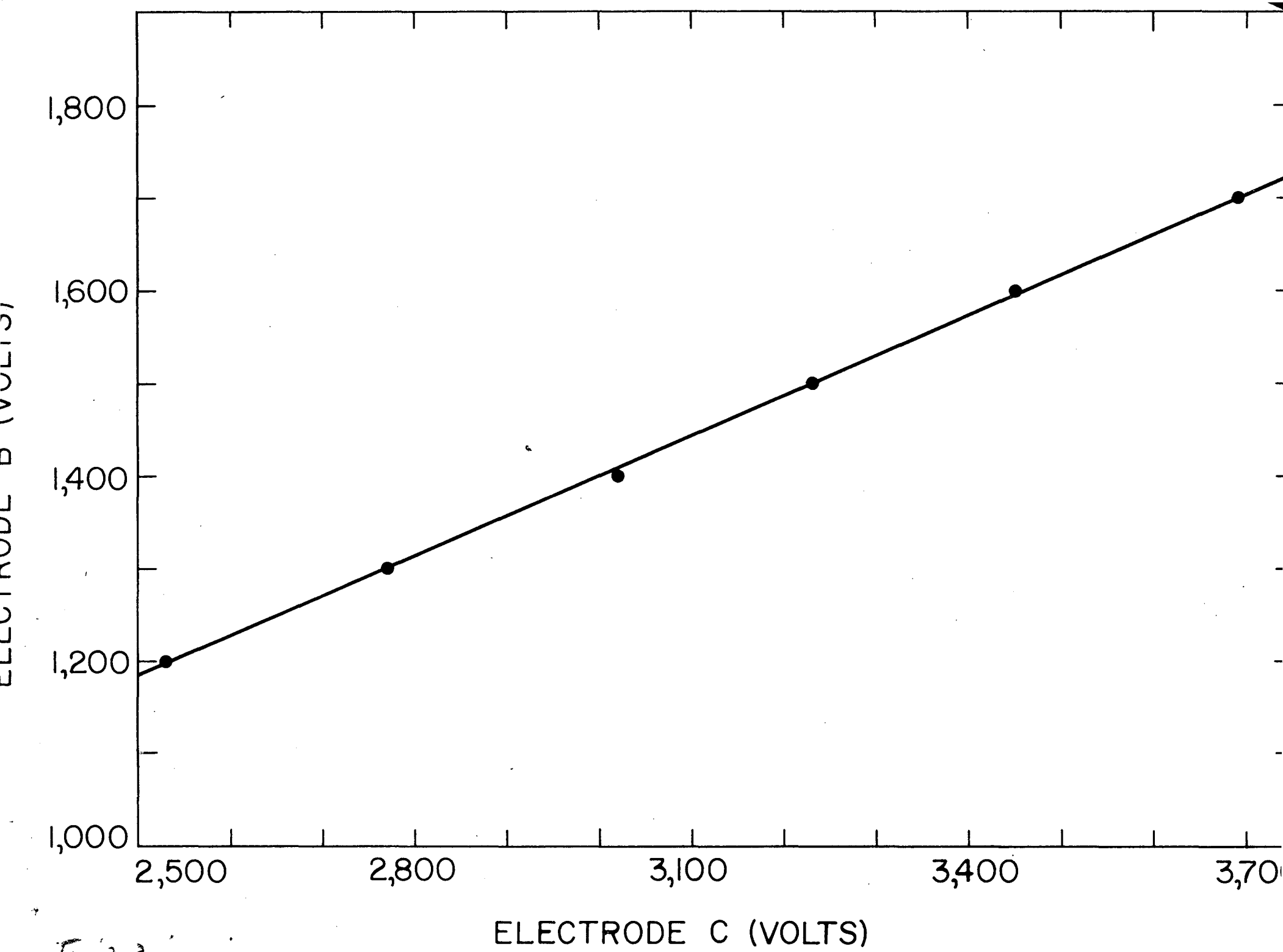
1,800
1,600
1,400
1,200
1,000
2,500
2,800
3,100
3,400
ELECTRODE C (VOLTS)

Fig. 3

23944-1

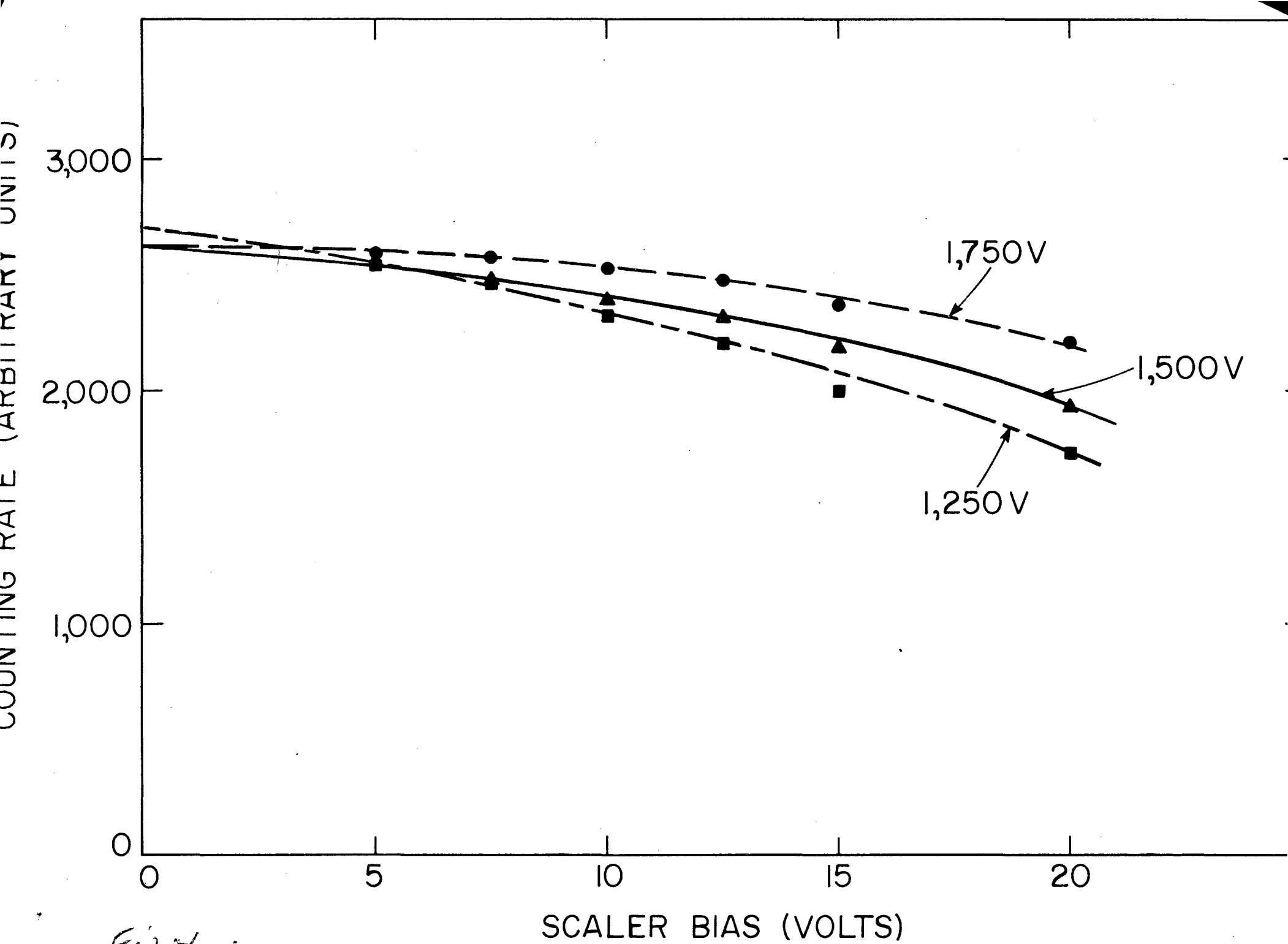
COUNTING RATE (ARBITRARY UNITS)
3,000
2,000
1,000
0
0
5
10
15
20
SCALER BIAS (VOLTS)
1,750V
1,500V
1,250V

Fig. 4

23989-1

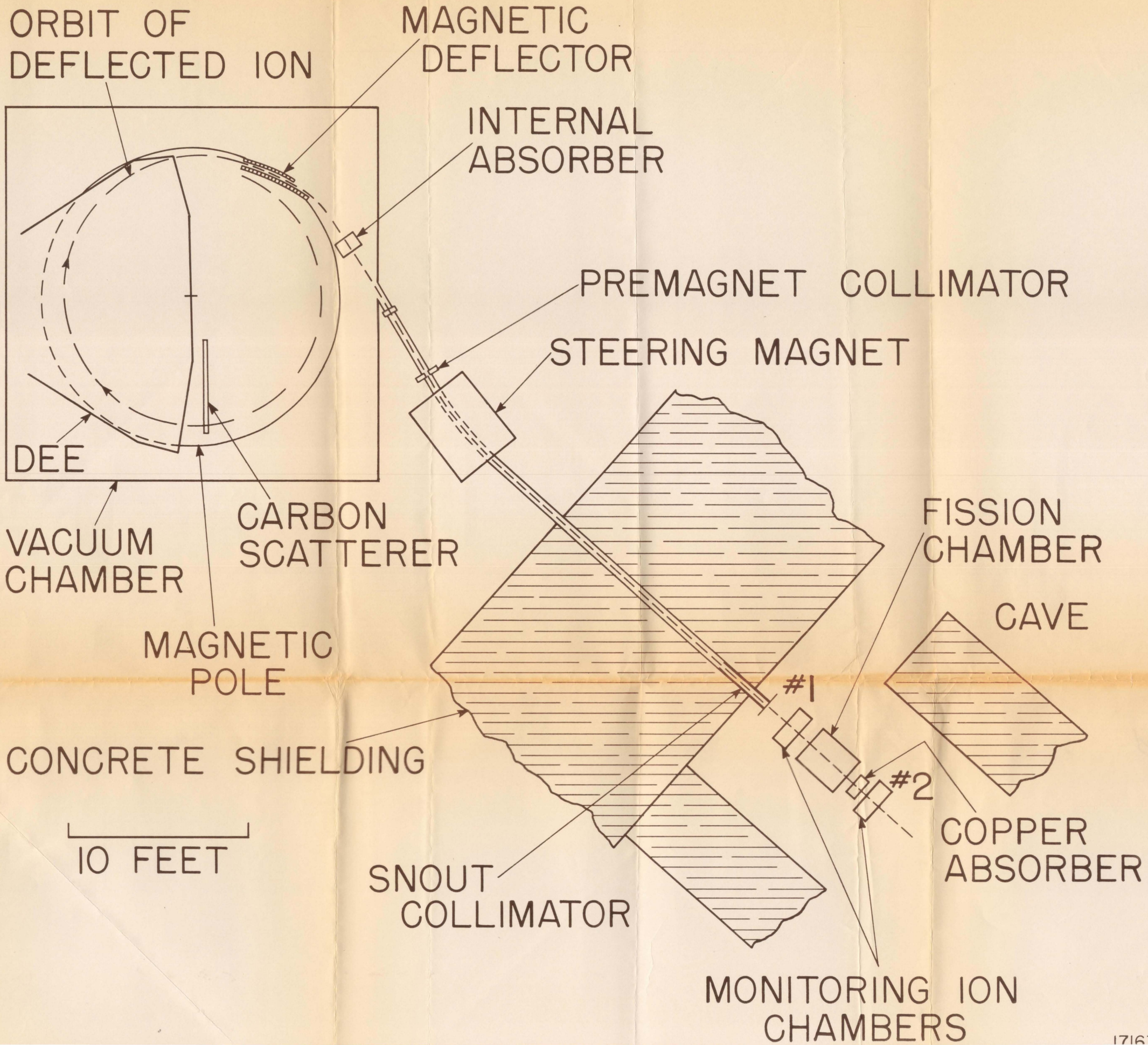
ORBIT OF DEFLECTED ION
MAGNETIC DEFLECTOR
INTERNAL ABSORBER
PREMAGNET COLLIMATOR
STEERING MAGNET
DEE
VACUUM CHAMBER
CARBON SCATTERER
MAGNETIC POLE
FISSION CHAMBER
CAVE
#1
#2
CONCRETE SHIELDING
10 FEET
COPPER ABSORBER
SNOUT COLLIMATOR
MONITORING ION CHAMBERS

17163-3-1

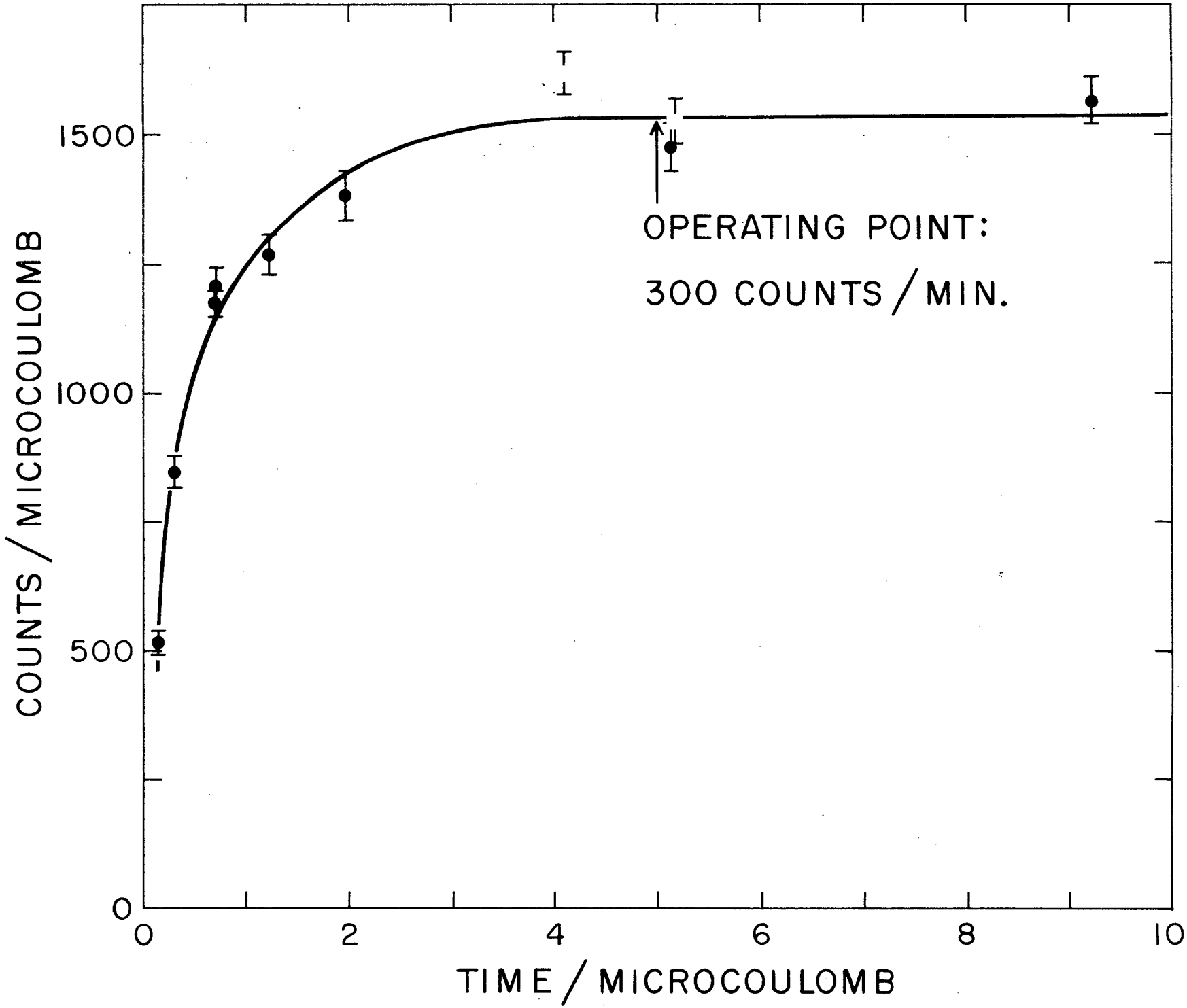
COUNTS / MICROCOULOMB
1500
1000
500
0
0
2
4
6
8
10
TIME / MICROCOULOMB
OPERATING POINT:
300 COUNTS / MIN.

Fig. 6

24051-1

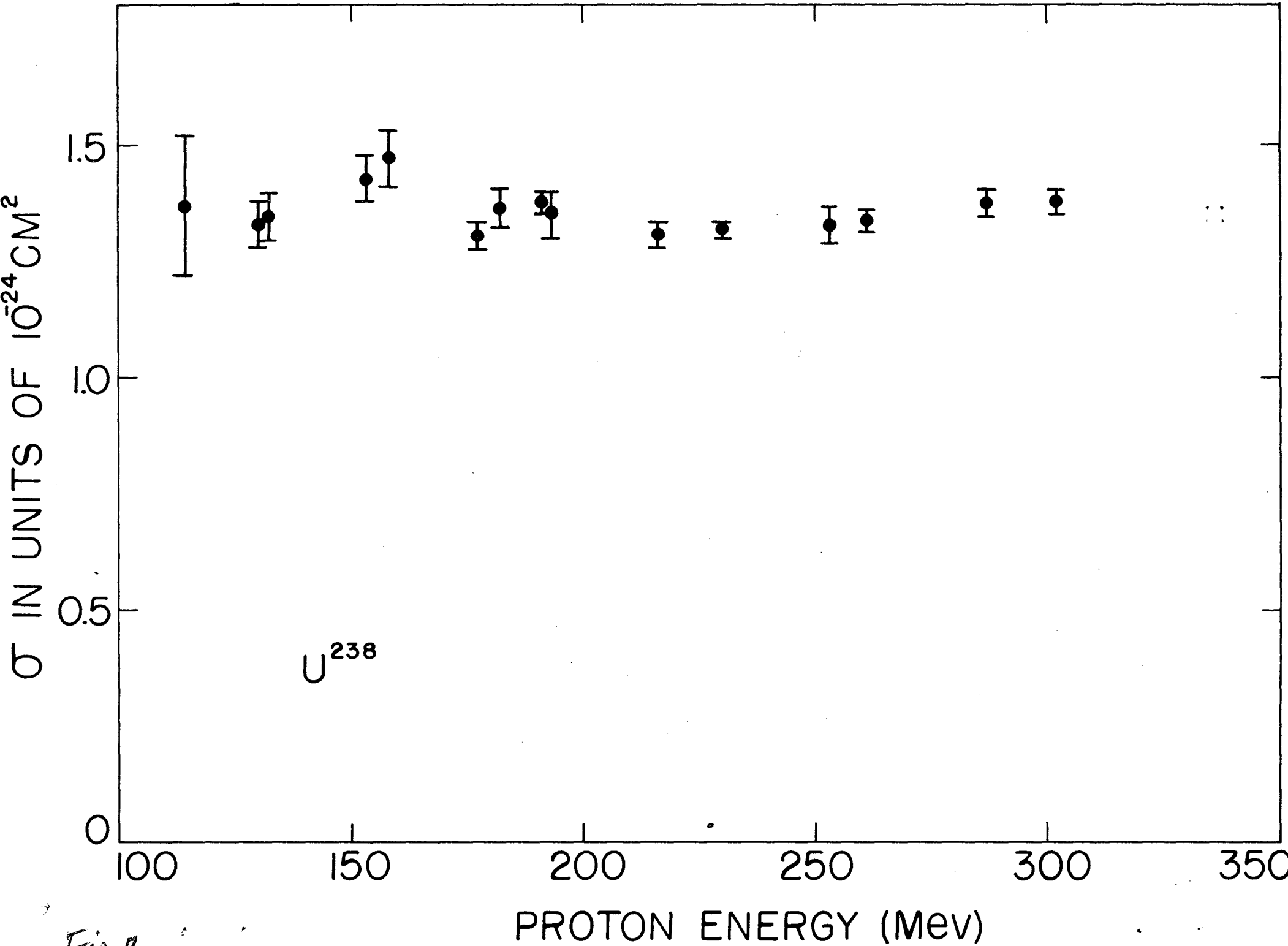
σ IN UNITS OF 10^{-24} CM^2
1.5
1.0
0.5
0
U^{238}
100
150
200
250
300
350
PROTON ENERGY (Mev)

Fig. 7

23994-1

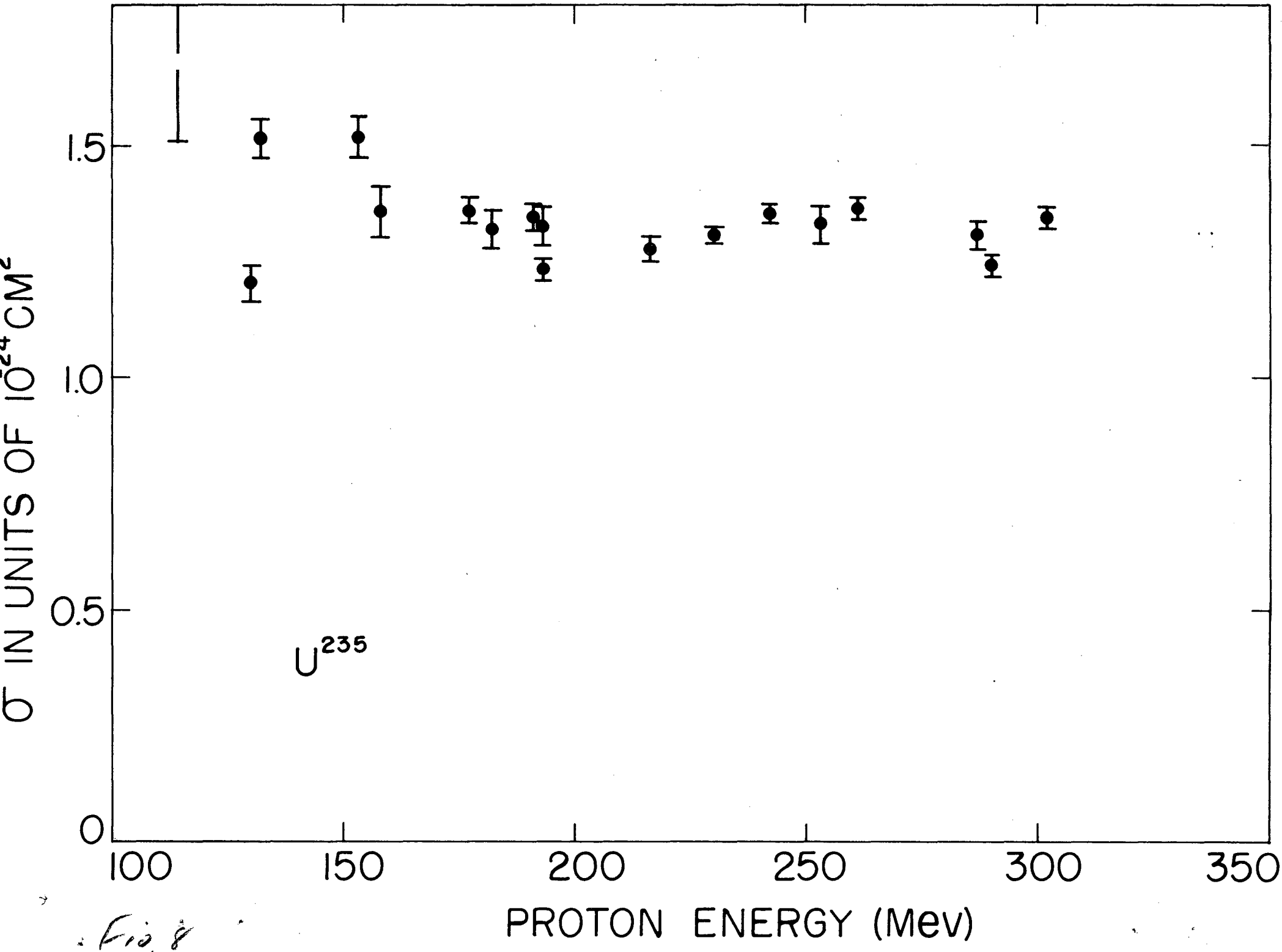
σ IN UNITS OF 10^{-24} CM^2
1.5
1.0
0.5
0
100
150
200
250
300
350
PROTON ENERGY (Mev)
U^{235}

Fig. 8

23993-1

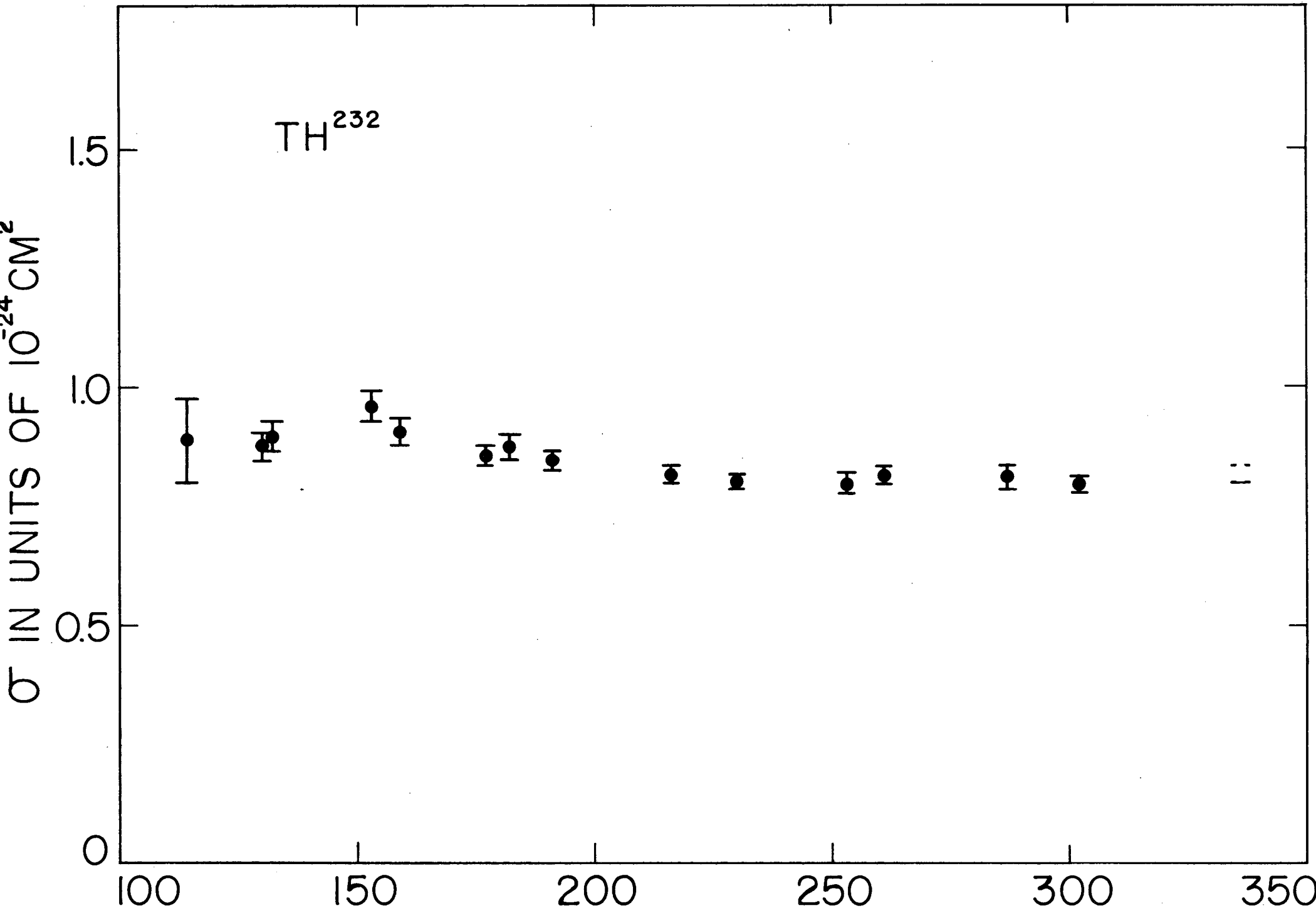
TH232
1.5
1.0
0.5
0
σ IN UNITS OF 10-24 CM2
100
150
200
250
300
350
PROTON ENERGY (Mev)

Fig. 9

23992-1

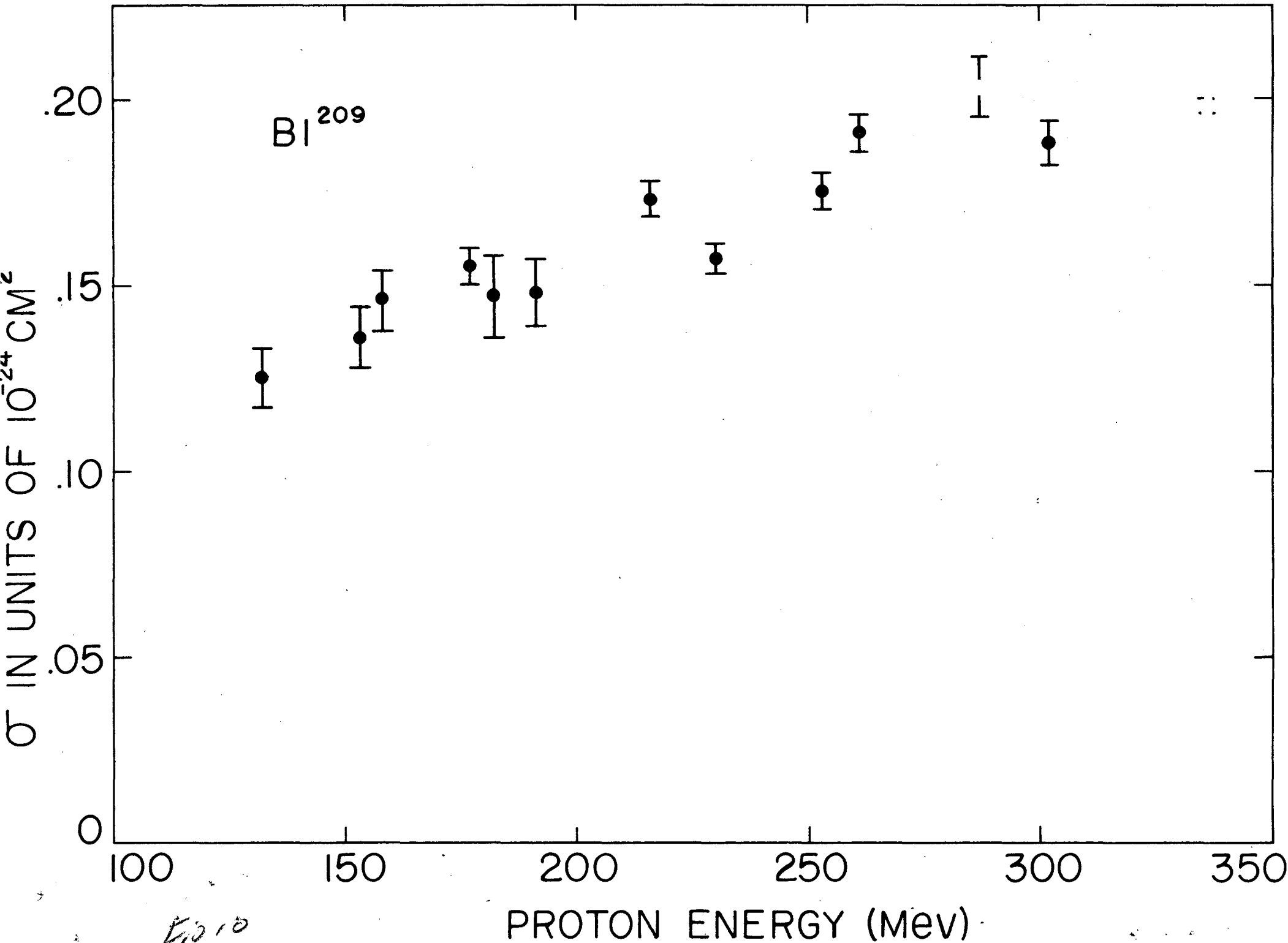

Fig. 10

23991-1

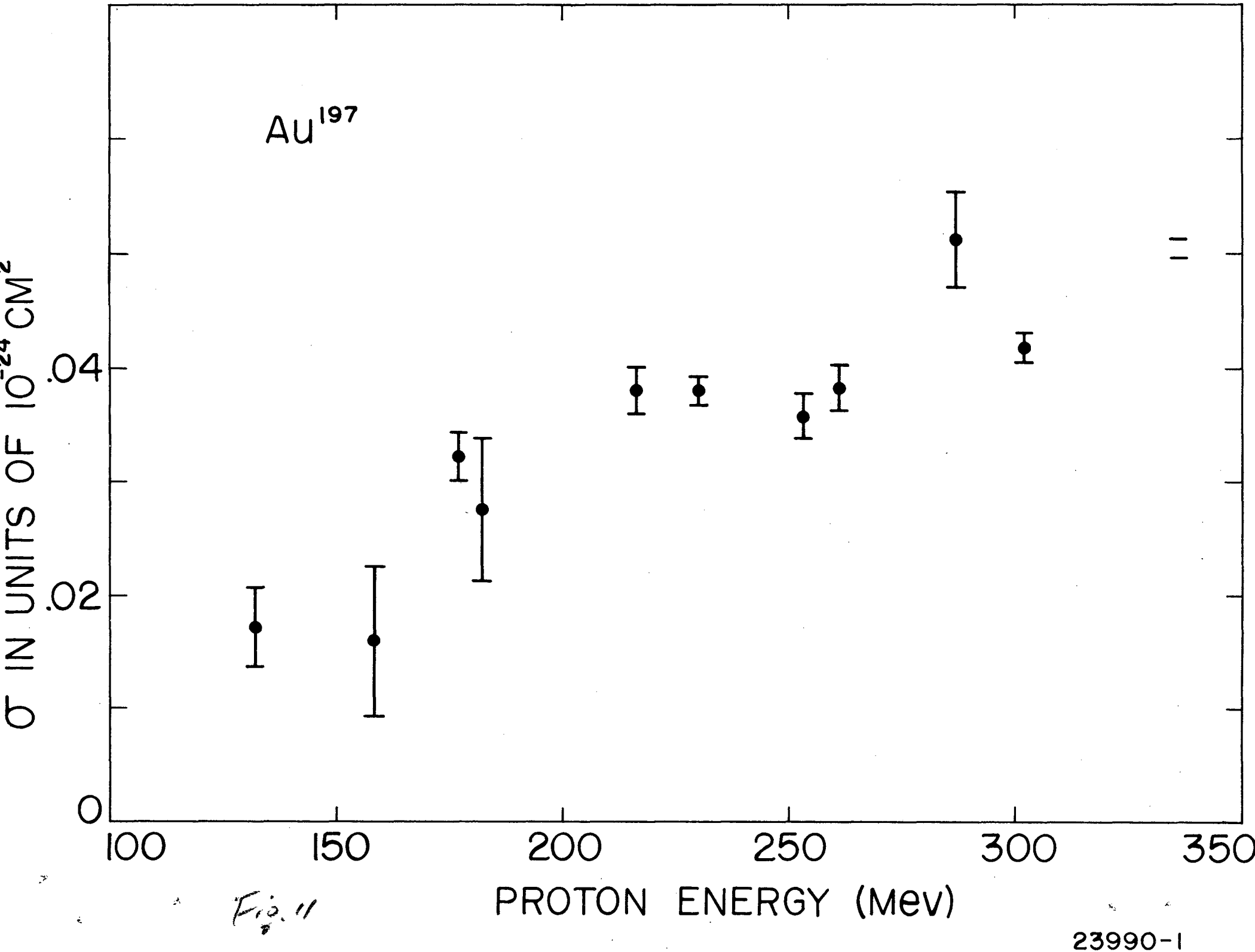
Au197
σ IN UNITS OF 10-24 CM2
.04
.02
0
100
150
200
250
300
350
PROTON ENERGY (Mev)
23990-1

Fig. 11

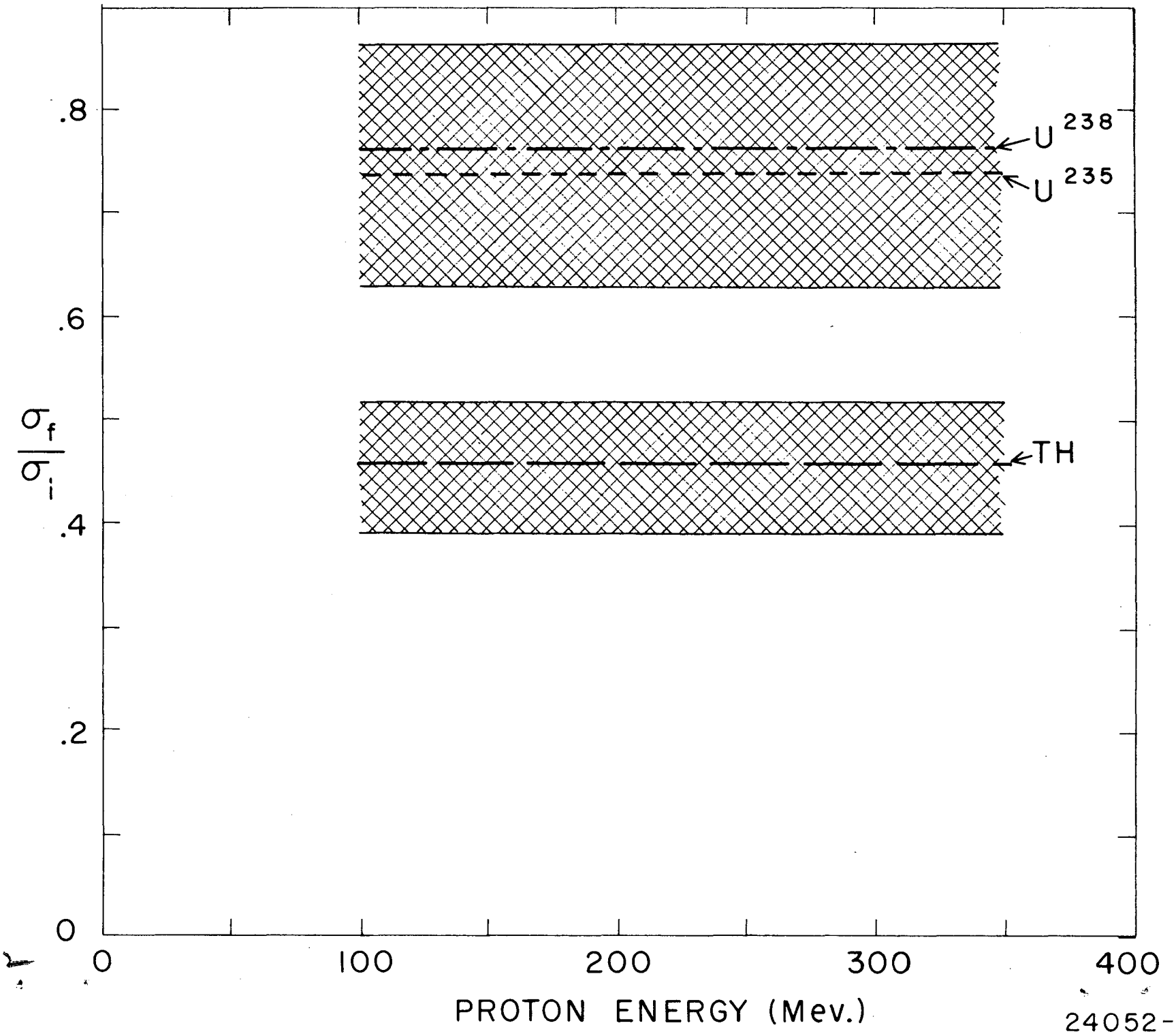

Fig 12

24052-1

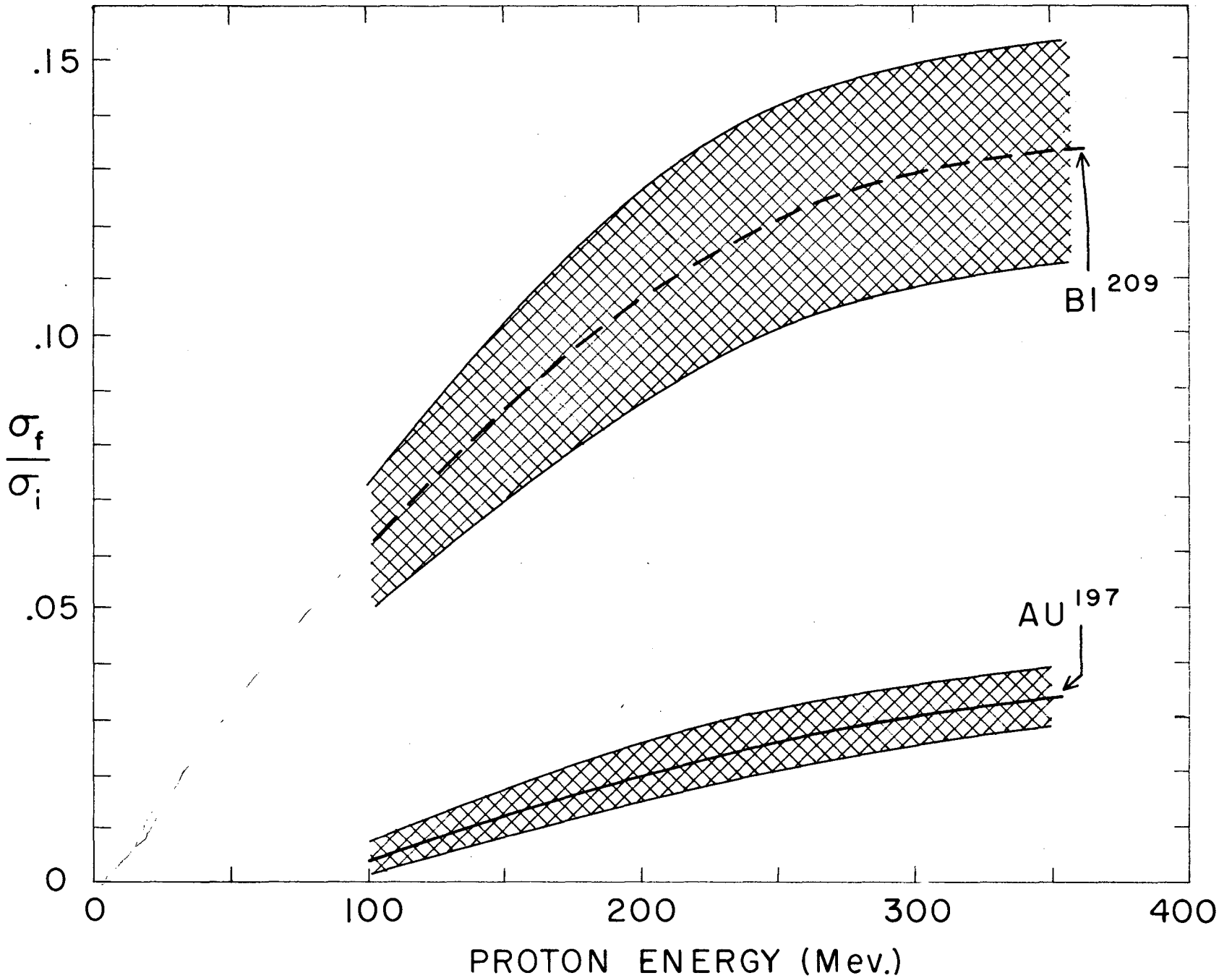

Fig. 13

24053-1